Bull. Fish. Sci. Hokkaido Univ.
74(1), 13–22, 2024.
DOI 10.14943/bull.fish.74.1.13

Size spectra of phytoplankton and zooplankton in the western North Pacific during May: A comparison between subarctic and transitional domains

Li WANG[1),2)], Xufa MA[1)], Dongwoo KIM[2)], Kohei MATSUNO[2),3)] and Atsushi YAMAGUCHI[2),3)]

(Received 29 January 2024, Accepted 4 April 2024)

Abstract

Size spectra data from marine phytoplankton and zooplankton can provide deep insights into material transfer in lower trophic levels. In this study, we quantified size spectra data of phytoplankton and zooplankton in the subarctic (SA) and transitional (TR) domains in the western North Pacific during May 2023. Phytoplankton and zooplankton data were obtained using FlowCam and ZooScan imaging instruments, respectively. Significantly normalized biovolume size spectra (NBSS) were detected for all samples in both taxa. There were no regional differences in abundance or biovolume. A large regional pattern was detected for the size spectra of phytoplankton at the sea surface. In samples from the TR, the mean biovolume per cell was larger, the slope of NBSS was flatter, and the size diversity was higher than in those in the SA. The NBSS slope and size diversity both showed higher variation in phytoplankton than in zooplankton. Based on the combination of phytoplankton and zooplankton at the same station, NBSS covering the whole planktonic size range are presented. In both taxa, a large discrepancy, e.g., missing NBSS area, was present from 10^{-5} to 10^{-1} mm^3 $ind.^{-1}$ in the biovolume. Methods to fill this gap in future studies are discussed.

Key words: Phytoplankton, Zooplankton, NBSS, Size diversity, Western North Pacific

Introduction

Normalized biomass size spectra (NBSS) are an index of the marine lower trophic level energy or material transfer to the higher trophic level organisms (Zhou, 2006 ; Zhou et al., 2009). The intercept of NBSS provides information on the amount of biomass within the food web, and the slope of NBSS indicates the trophic transfer efficiency or turnover rate (Zhou, 2006). The NBSS slope is known to vary with grazing intensity (Gómez-Canchong et al., 2012 ; Chang et al., 2013) and respond to both the production of phytoplankton and the predation by zooplankton (Moore and Suthers, 2006). Recently, spatial and temporal changes (Baird et al., 2008 ; Espinasse et al., 2014 ; Marcolin et al., 2015 ; Garcia-Oliva et al., 2022), as well as day/night changes (Suthers et al., 2006), and vertical changes (Liu et al., 2021) in size spectra have been evaluated using the NBSS from worldwide oceans. Traditionally, mesozooplankton NBSS were usually assessed using optical plankton counter (OPC) measurements (Yurista et al., 2005 ; Huntley et al., 2006 ; Sourisseau and Carlotti, 2006). The OPC and the laser OPC (LOPC) have been used to compare zooplankton NBSS (Herman and Harvey, 2006). Such a comparison has also been done for mesozooplankton between an Underwater Vision Profiler 5 (UVP5) and traditional net tows (200 μm mesh size) (Forest et al., 2012). For phytoplankton, size distributions have been compared between a laser diffractometer (LISST-100X), an electrical impedance particle sizer (Coulter Counter), and a particle imaging system (FlowCam) (Reynolds et al., 2010). To cover a wide size range, Flow Cytometry, FlowCam, and ZooScan have been used together in the last decade to estimate the NBSS of the whole plankton community (from microbes to macrozooplankton predators) (Vandromme et al., 2012).

Obtaining NBSS from the whole plankton community is the goal for such a size spectra study. NBSS from heterotrophic bacteria to zooplankton have been evaluated by combining different techniques: flow cytometry, inverse microscopy, FlowCam, and ZooScan (Romagnan et al., 2015 ; Kydd et al., 2018). However, because of the limitations of the instruments, the NBSS obtained from various methods have shown discrepancies (Nogueira et al., 2004 ; Schultes and Lopes, 2009 ; Jakobsen and Carstensen, 2011 ; Forest et al., 2012 ; Vandromme et al., 2014 ; Kwong

[1)] *College of Fisheries, Huazhong Agricultural University, PR China*
(中華人民共和国 華中農業大学)
[2)] *Laboratory of Marine Biology, Graduate School of Fisheries Sciences, Hokkaido University*
(北海道大学大学院水産科学院海洋生物学分野)
[3)] *Arctic Research Center, Hokkaido University*
(北海道大学北極センター)

and Pakhomov, 2021). Interestingly, the NBSS slopes combining phytoplankton, mesozooplankton, and macrozooplankton using FlowCam and ZooScan methods have been reported to be flatter than the single zooplankton NBSS slope (Zhang et al., 2019). The NBSS for various trophic groups can be obtained only from the combination of each trophic group (Sprules and Stockwell, 1995). A combination of size diversity and NBSS has also provided interesting insight into the plankton size spectra (Sun et al., 2021). However, such studies are scarce despite their importance.

In the western North Pacific, there have been several studies on the size spectra of the whole plankton community (bacteria, phytoplankton, protozooplankton, and metazooplankton) from subarctic to subtropical regions (Yamaguchi et al., 2002 ; 2004). For several coastal areas, seasonal changes in mesozooplankton NBSS slope have also been reported (Hikichi et al., 2018 ; Teraoka et al., 2022). For the vertical changes, the compositions at 0–150 m and 150–500 m depths have been reported in the Oyashio region based on year-round collected zooplankton samples (Yamaguchi et al., 2014). While such information is valuable, most of these studies have targetted only zooplankton, and most of the data were derived from OPC instruments (Yokoi et al., 2008 ; Matsuno and Yamaguchi, 2010 ; Fukuda et al., 2012 ; Sato et al., 2015). The combination of phytoplankton with zooplankton NBSS and the elimination of detritus from the particle data have not been made in this region.

The aim of our study was to obtain NBSS for both phytoplankton and mesozooplankton in the subarctic (SA) and transitional (TR) domains in the western North Pacific during May 2023. For quantification of size spectra of the two plankton groups, we applied two imaging devices : FlowCam for phytoplankton and ZooScan for mesozooplankton. We compared NBSS parameters (slope and intercept) and the size diversity of each taxon between the two domains. For phytoplankton, vertical changes in size spectra were evaluated using samples collected from three depths (0, 30, and 50 m). Based on the results of this study, we propose methods to assess the size spectra covering the whole plankton community in future studies.

Materials and methods

Field sampling

Plankton samplings were conducted at six stations in the western North Pacific aboard the T/S *Oshoro-Maru* during 14–19 May 2023 (Table 1, Fig. 1). Samplings were made both day and night (3 stations during the day, 2 at night, and 1 at dusk) (Table 1). For phytoplankton, 1-L water samples were collected in dark bottles from three depths (0, 30, and 50 m) using a bucket (0 m) or rosette of Niskin bottles mounted on a CTD. Zooplankton samples were collected in vertical tows of a Quad-NORPAC net (mesh size of 335 μm, mouth diameter of 45 cm, Hama et al., 2019) from 150 m to the sea surface. The NORPAC nets were equipped with a flowmeter (Rigosha & Co., Ltd.) at the net mouth ring to register the volume of filtered water. Data of the filtered volume (m^3) of each sample are shown in Table 1. The zooplankton samples were preserved by adding 5% borax-buffered formalin (v/v) on board immediately after collection. Temperature, salinity, and fluorescence were measured by a fluorometer mounted on the CTD (SBE 911 plus ; Sea-Bird Scientific).

FlowCam analysis

Using the collected non-preserved water samples, the size of phytoplankton was measured using FlowCam (8100, Fluid Imaging Technologies Inc.) as soon as possible after collection on board. For measurement, a 5-mL water sample was inserted into the FlowCam using a 10-mL tube. The phytoplankton were measured with a ×10 objective lens in AutoImage mode, and the detection limit was 2 μm of equivalent spherical diameter (ESD). Each sample was pumped through a chamber with a cross-section of 100 μm × 700 μm. The total volume of the examined samples was 1.78–3.35 mL (mean ± 1sd : 2.84 ± 0.31 mL). Particle images outside the 4–100 μm ESD range were not captured. Invalid images (including bubbles, repeated images, detritus, and fragments of cells) were removed before data analysis.

ZooScan analysis

In the land laboratory, zooplankton images of the formalin-

Table 1. Sampling data on phytoplankton (0, 30, 50 m depth) and zooplankton (0–150 m depth) at six stations in the western North Pacific during 14–19 May 2023. Sampling times at each station are shown as D (day) or N (night). For zooplankton, data on the filtered volume of the plankton net are also shown. – : dusk.

Station	Position		Local time		D/N	Net filtered volume (m^3)
no.	Lat. (N)	Lon. (E)	Date	Hour		
1	41°33.01′	151°02.41′	14-May	20 : 00	N	28.18
2	42°04.97′	151°37.07′	15-May	14 : 17	D	22.46
3	42°18.84′	152°02.73′	15-May	20 : 21	N	23.71
4	40°00.00′	145°00.00′	18-May	12 : 07	D	23.19
5	40°29.79′	145°00.03′	19-May	11 : 40	D	23.11
6	40°59.72′	144°59.83′	19-May	18 : 25	–	24.02

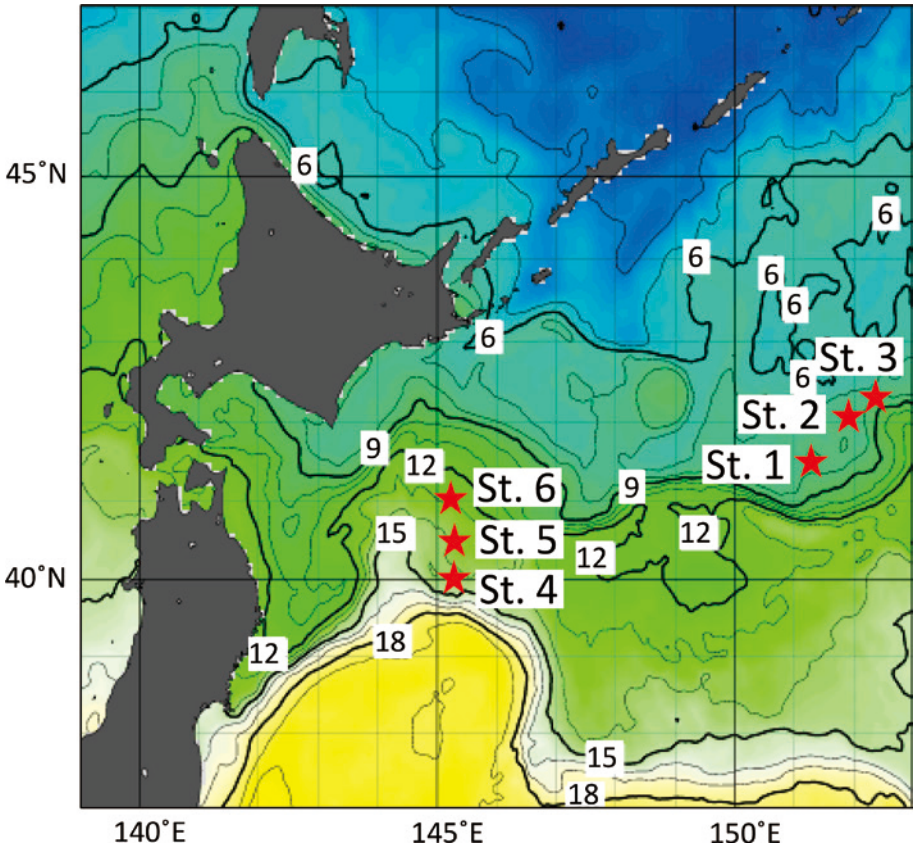

Fig. 1. Locations of sampling stations (St. 1–6, red stars) in the western North Pacific during 14–19 May 2023 and sea surface temperature during the study period (data derived from the Japan Meteorological Agency).

preserved samples were scanned with a ZooScan system (Hydrooptic Inc.) based on the method of Gorsky et al. (2010). Before each measurement, background measurements were made with deionized water. Zooplankton subsamples of 1/2 to 1/64 (depending on the amount of the sample) were made using a Motoda sample splitter (Motoda, 1959) and scanned. The obtained images were separated into individual images using ZooProcess software. The zooplankton images were digitized at 2400 dpi resolution, at which one pixel corresponded to 10.6 µm. The obtained images were uploaded to the website EcoTaxa (http://ecotaxa.obs-vlfr.fr/prj/), which uses machine learning to identify plankton images, as described in Picheral et al. (2017). The taxonomic groups and species identified in this study included Amphipoda, Appendicularia, Chaetognatha, Cladocera, Cnidaria, Copepoda, Echinoidea, Euphausiacea, Foraminifera, Harpacticoida, Hydrozoa, Mollusca, Ostracoda, Phaeodaria, Polychaeta, copepod nauplii, and eggs.

ZooScan provides the body length (major axis) and width (minor axis) of the object (Gorsky et al., 2010). The volume of the ellipse (*Volume* : mm^3) was calculated using the major axis length (L_{major} : mm) and the minor axis width (L_{minor} : mm) :

$$Volume = 4 / 3 \times \pi \times \left(L_{major} / 2\right) \times \left(L_{minor} / 2\right)^2$$

From the volume of the ellipse, the ESD of the object was calculated.

$$ESD = 2 \times \left(\sqrt[3]{\frac{Volume \times 3}{4\pi}} \right)$$

The abundance (N : ind. m^{-3}) was calculated from the number of particles (n) and the volume of filtered water (F : m^3) :

$$N = n / \left(F \times s\right)$$

where s is the split factor of the samples used for the ZooScan measurement.

The biovolume (B : mm^3 m^{-3}) was also calculated from the *Volume* (mm^3), F, and s using the following equation :

$$B = \frac{Volume}{F \times s}$$

The mean biovolume per individual (M : mm^3 $ind.^{-1}$) was also calculated from biovolume (B) and abundance (N) using the following equation :

$$M = B / N$$

Normalized biovolume size spectra

To obtain normalized biomass size spectra (NBSS), we

used the biovolume data on phytoplankton (derived from FlowCam) and zooplankton (derived from ZooScan) at size ranges of 4–100 μm ESD binned in 1 μm intervals (= 96 size classes, phytoplankton) and 0.2–5.0 mm ESD binned in 0.1 mm intervals (= 48 size classes, zooplankton), respectively. Biovolume was divided by the biovolume interval (Δbiovolume [mm^3]) and log_{10}-transformed. Specifically, we used log_{10} plankton biovolume (mm^3) in each size class for the X-axis and log_{10} plankton biovolume ($mm^3\ m^{-3}$) / Δbiovolume (mm^3) for the Y-axis. Then, the NBSS linear model was calculated as follows :

$$Y = aX + b$$

where a and b are the slope and intercept of the NBSS, respectively.

Size diversity

The size diversity of the plankton community was calculated by the Shannon–Weaver index formula (Shannon and Weaver, 1963) :

$$Size\ diversity = -\sum_{i=1}^{c} P_i \ln P_i$$

where c is the total number of size categories, and P_i is the proportion of the size class i in the total biovolume.

Statistical analysis

Since hydrographic conditions at six stations were classified into two regions, the Mann–Whitney U-test was used to compare abundance, biovolume, biovolume per cell (phytoplankton) or individual (zooplankton), NBSS slopes, intercept, and size diversities between the two regions. For both phytoplankton and zooplankton, linear fittings were examined to explore the relationship between NBSS slope and size diversity.

Results

Hydrography

The vertical changes in temperature and fluorescence, and the T–S diagram at the six stations are shown in Fig. 2. Temperature at the sea surface was 3.0–18.1°C and decreased with increasing depth (Fig. 2a). Vertical temperature changes were more prominent at St. 4–6 than at St. 1–3, and a thermocline was observed around 20–25 m at St. 4–6 (Fig. 2a). At all stations, fluorescence peaked at 14–33 m depths with no apparent differences between stations (Fig. 2b). Based on the T–S diagram, the stations were classified into cold and low salinity stations in the subarctic (SA) domain (St. 1–3) and warm and saline stations in the transition (TR) domain (St. 4–6) (Fig. 2c). These classifications corresponded well with the sea surface temperature derived from satellite images (cf. Fig. 1).

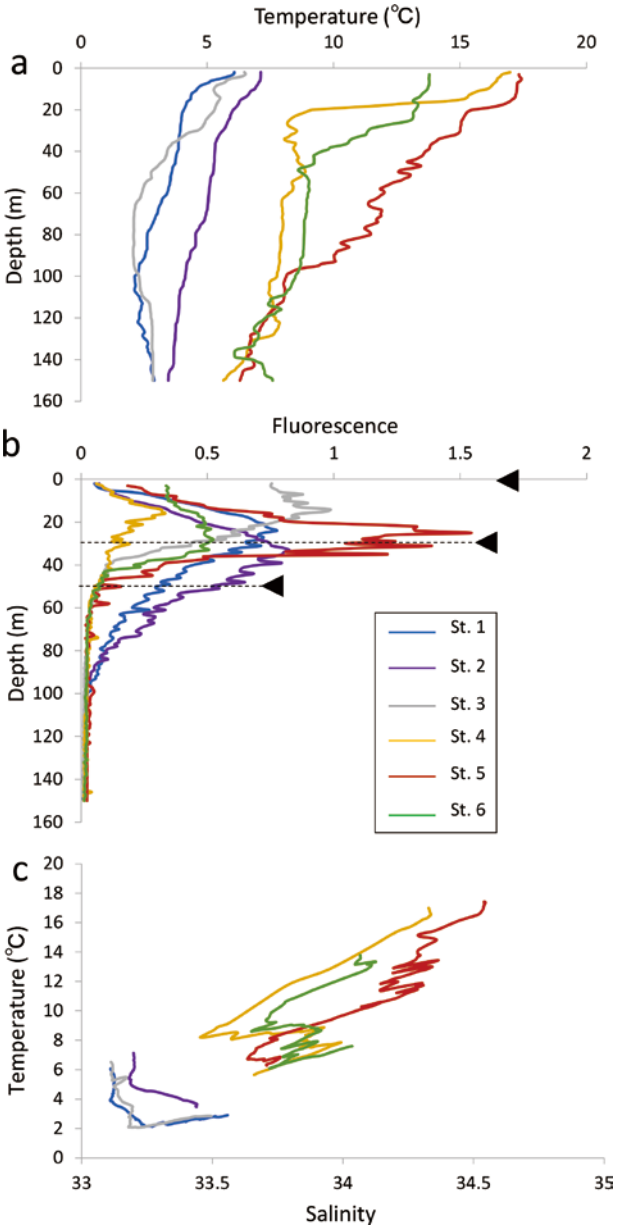

Fig. 2. Vertical changes in water temperature (a) and fluorescence (b) at 0–150 m depths at six stations ; T–S diagram at each station (c) in the western North Pacific during 14–19 May 2023. Dashed lines and solid triangles in (b) represent the water sampling depths (0, 30, 50 m) for phytoplankton analyses.

Abundance and biovolume

The mean phytoplankton cell density at each sampling depth in the two regions ranged between 77 and 287 cells mL^{-1} (Table 2). In both regions, phytoplankton cell density was the highest at the sea surface (0 m) and decreased with increasing depth. Regional differences were not detected for phytoplankton abundance at each depth. Phytoplankton biovolume ranged between 12 and 45 $mm^3\ m^{-3}$ (Table 2). Regional differences were not seen for phytoplankton biovol-

Table 2. Comparison of abundance, biovolume, mean biovolume per cell/individual, NBSS slope, intercept, and size diversity between the subarctic stations (SA, St. 1–3) and transitional domain stations (TR, St. 4–6) in the western North Pacific during 14–19 May 2023. Values are mean ± 1sd. Differences between the regions were tested by the Mann–Whitney *U*-test. * : $p < 0.05$, ** : $p < 0.01$, *** : $p < 0.001$, ns : not significant. The superscript alphabets (a–d) represent the differences in units. Thus, a : cells ml^{-1}, b : ind. m^{-3}, c : μm^3 $cell^{-1}$, and d : $\times 10^{-3}$ mm^3 $ind.^{-1}$.

Taxa/depth	Region	Abundance	Biovolume (mm^3 m^{-3})	Mean biovolume per cell/individual	NBSS slope	NBSS intercept	Size diversity
Phytoplankton							
0 m	SA	287.08±197.76[a]	18.96±19.80	63.87±31.01[c]	−0.93±0.05	0.50±0.54	2.03±0.13
	TR	165.30±26.60[a]	32.72±5.46	197.92±6.28[c]	−0.65±0.01	2.65±0.03	2.73±0.01
	U-test	ns	ns	**	***	**	***
30 m	SA	124.58±35.93[a]	16.10±5.72	134.33±57.12[c]	−0.73±0.18	1.83±1.10	2.33±0.19
	TR	141.86±33.05[a]	45.29±17.29	316.75±69.44[c]	−0.51±0.06	3.41±0.35	2.82±0.08
	U-test	ns	ns	*	ns	ns	*
50 m	SA	77.14±16.55[a]	12.36±3.42	166.31±65.10[c]	−0.56±0.20	2.79±1.31	2.49±0.27
	TR	79.66±19.05[a]	24.62±17.25	287.26±140.54[c]	−0.47±0.08	3.40±0.58	2.68±0.18
	U-test	ns	ns	ns	ns	ns	ns
Zooplankton							
0–150 m	SA	1,415±1,466[b]	144.39±106.14	132.18±59.91[d]	−0.42±0.10	0.88±0.37	2.54±0.11
	TR	948±470[b]	78.75±18.80	91.73±26.26[d]	−0.52±0.07	0.90±0.16	2.64±0.19
	U-test	ns	ns	ns	ns	ns	ns

ume at each depth. Vertical changes in phytoplankton biovolume were unclear. As a consequence, the mean biovolume per cell was the lower at the surface (0 m) than at deeper layers (30 m and 50 m) (Table 2). The mean phytoplankton biovolume was smaller in the SA (63–134 mm^3 $cell^{-1}$) than in the TR (197–316 mm^3 $cell^{-1}$), especially at shallower depths (0 and 30 m).

Mean zooplankton abundance at the two regions was 948 ind. m^{-3} (TR) and 1415 ind.m^{-3} (SA) and showed no significant regional differences. The mean zooplankton biovolume was 78 mm^3 m^{-3} (TR) and 144 mm^3 m^{-3} (SA) and did not vary between the regions. The mean biovolume per individual was 91×10^{-3} mm^3 $ind.^{-1}$ in the TR and 132×10^{-3} mm^3 $ind.^{-1}$ in the SA, and showed no significant regional differences.

NBSS and size diversity

NBSS of phytoplankton and zooplankton at three stations in the SA and three stations in the TR are shown in Fig. 3. Since the sizes measured by the two instruments (FlowCam and ZooScan) varied greatly, large discrepancies were observed between NBSS on phytoplankton and zooplankton for all stations (Fig. 3). While such shortcomings were present, clear regional differences were observed in NBSS of phytoplankton at shallower depths especially at the sea surface (0 m). Thus, for phytoplankton at 0 m, the NBSS slope was steep in the SA and moderate in the TR (Table 2). The NBSS intercept of the sea surface phytoplankton was low in the SA and high in the TR. The size diversity of phytoplankton also varied with region. Thus, the size diversity of phytoplankton was low in the SA, especially at 0 m and 30 m, while the size diversity was high in the TR at these depths. Except for phytoplankton at shallower depths (0 m), both NBSS and size diversity showed no regional differences for phytoplankton at deeper depths (50 m) and zooplankton at 0–150 m (Table 2).

Comparison between NBSS and size diversity

In this study, we used two indices (NBSS and size diversity) to express the size spectra of phytoplankton and zooplankton. The scatter plots between NBSS slope and size diversity and their regressions at the three depths for phytoplankton and zooplankton are shown in Fig. 4. Through the taxa and depths, the NBSS slope was moderate under the high size diversity conditions. Significant regressions between the NBSS slope and size diversity were present for phytoplankton at the three depths ($p < 0.05$). From the scatter plots, regional changes in the NBSS slope and size diversity were also marked. For phytoplankton at the sea surface, the steeper NBSS slope and lower size diversity in the SA than in the TR were prominent (Fig. 4a). For phytoplankton at 30 m, the size diversity was lower in the SA than in the TR (Fig. 4b).

Discussion

Abundance and biovolume

Phytoplankton abundance and biovolume data in the oceanic region of the western North Pacific are scarce. As a notable exception, Mochizuki et al. (2002) reported seasonal changes in phytoplankton cell abundance at Station KNOT (44°N, 155°E) based on year-round observations. Accord-

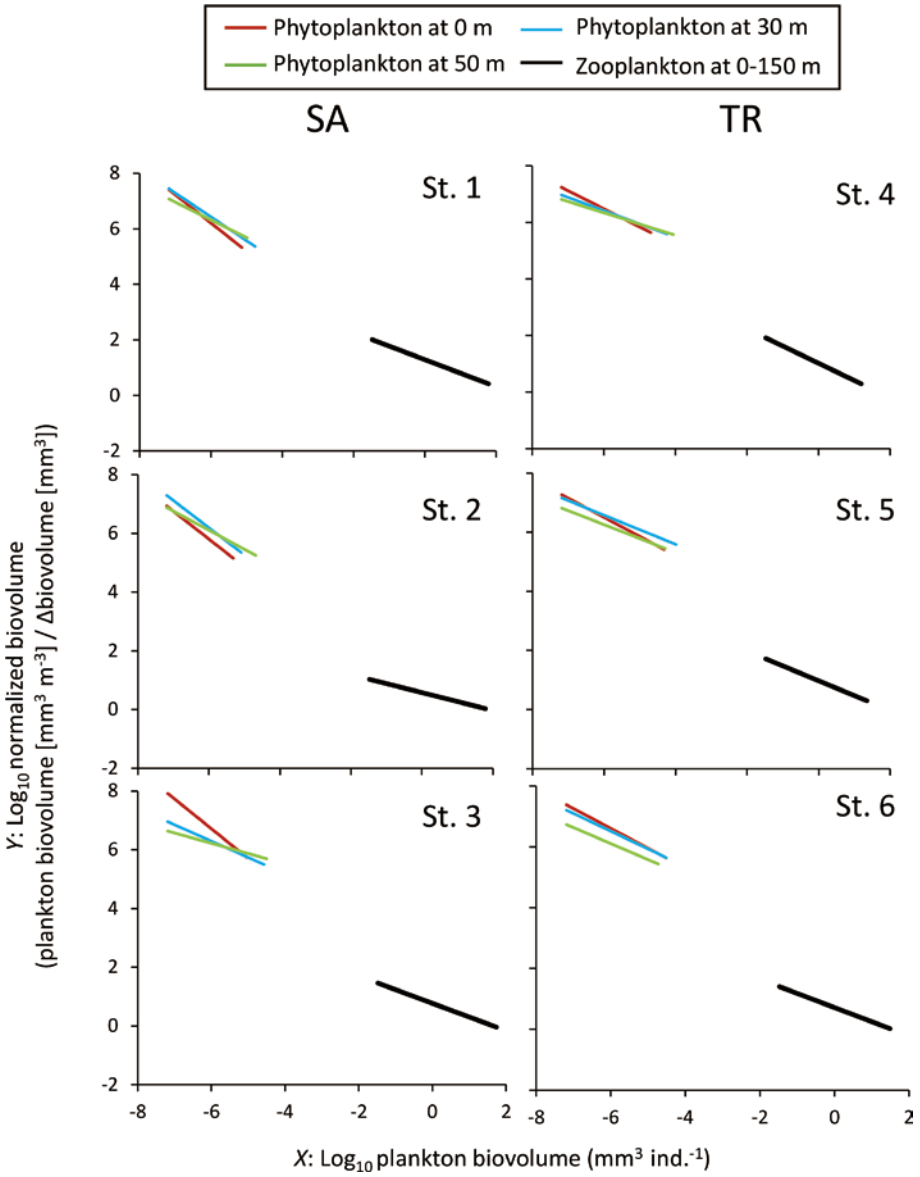

Fig. 3. Normalized biovolume size spectra (NBSS) of phytoplankton at three depths (0, 30, and 50 m) derived from FlowCam and of zooplankton at 0–150 m derived from ZooScan collected by NORPAC net at three stations (SA, St. 1–3) in the subarctic and three stations (TR, St. 4–6) in the transitional domain of the western North Pacific during 14–19 May 2023.

ing to Mochizuki et al. (2002), the highest cell density was ca. 60 cells mL^{-1} observed at the end of May (Fig. 3 of Mochizuki et al. 2002). This value is lower than the mean phytoplankton cell densities in the SA and TR regions in the present study (165–2817 cells mL^{-1}, Table 2). This discrepancy may have been due to the pre-treatment of the samples. Mochizuki et al. (2002) preserved their samples by adding 1% borax buffered formalin, concentrated the samples, and examined them under an inverted microscope. On the other hand, we measured non-preserved samples immediately after the collection on board. Since preservation by the buffered formalin can cause shrinkage of the cells, especially for the naked taxa, quantification was made only for the shelled taxa in Mochizuki et al. (2002). Concerning chlorophyll *a*, Mochizuki et al. (2002) reported low values throughout the year, with the highest value at 1.6 μg L^{-1}. Similar low values in this region were also confirmed by Matsumoto et al. (2016). Our fluorescence value in the present study was similar to values in these previous reports (Fig. 2b).

For zooplankton, abundance and biovolume data are available from various studies (Yamaguchi et al., 2004, 2017 ; Yokoi et al., 2008). Yokoi et al. (2008) reported that the mean abundance at 0–150 m depths was 352–580 ind. m^{-3}. The zooplankton abundance in the present study (948–1415 ind. m^{-3}, cf. Table 2) was higher than the values reported by Yokoi et al. (2008). Considering the high standard deviations in our results (Table 2), there seem to be no significant differences with the previously reported values. For zoo-

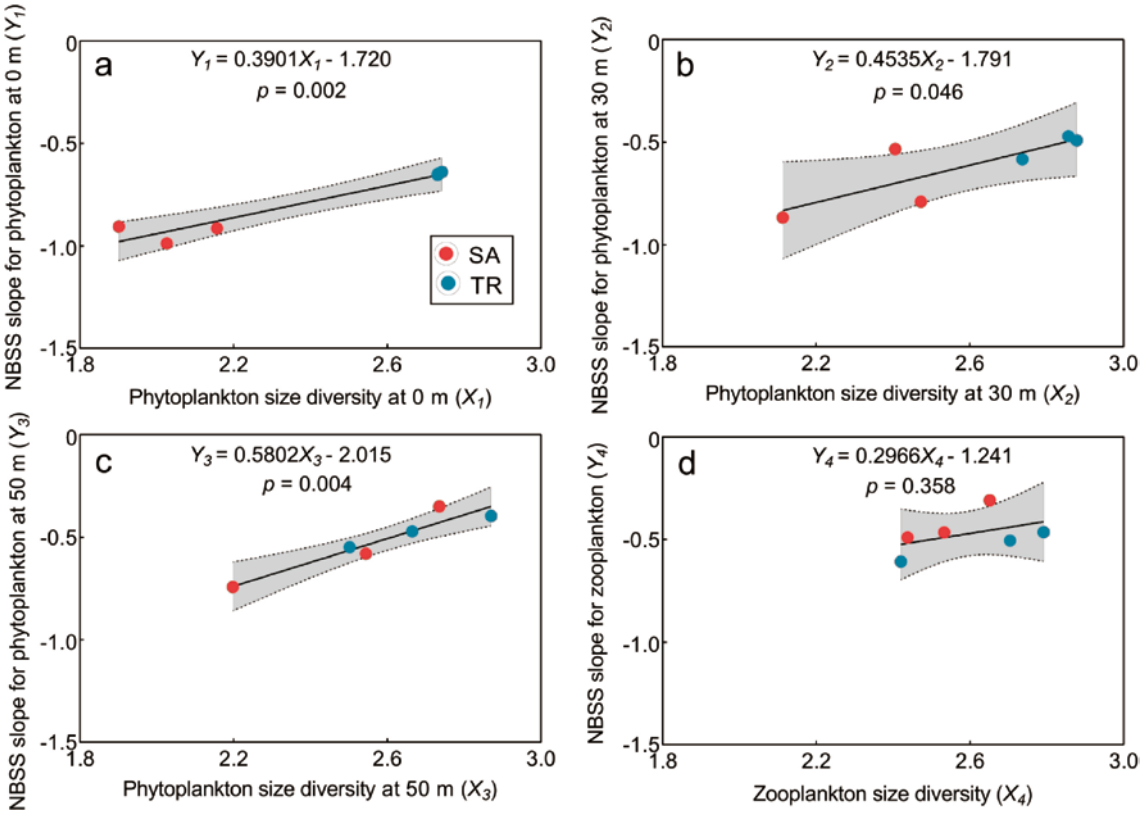

Fig. 4. The linear fittings between NBSS slope and size diversity for phytoplankton at three depths (a–c) and zooplankton (d) in the western North Pacific during 14–19 May 2023. The red and blue symbols represent stations in the subarctic (SA) and transitional domains (TR), respectively. The shaded areas indicate a 95% confidential interval.

plankton biomass, previous studies reported the biomass using other units such as carbon (Yokoi et al., 2008) or dry weight (Yamaguchi et al., 2017). If we convert our biovolume data to wet weight assuming that the zooplankton gravity was the same as water (=1 mg mm^{-3}), the estimated zooplankton wet weight is 78–144 mg WW m^{-3}. These values correspond well with the reported values in this region (Yamaguchi et al., 2004, 2017 ; Yokoi et al., 2008).

NBSS and size diversity

For all quantitative parameters of plankton (e.g., phytoplankton at three depths and net zooplankton at 0–150 m), significant regressions were present for NBSS (Fig. 3). For most parameters, significant correlations were also present between the NBSS slope and size diversity, i.e., moderate NBSS slope provided high size diversity (Fig. 4). These patterns correspond well with previously reported interactions between the NBSS slope and size diversity (Sun et al., 2021).

Within the four planktonic parameters, regional changes in NBSS and size diversity were present only for the phytoplankton at the sea surface (Table 2). As size characteristics of phytoplankton at the sea surface, the mean biovolume was larger in the TR than in the SA. Consequently, there was a more moderate NBSS slope and higher size diversity in the TR (Table 2). While these regional differences in phytoplankton size are interesting and highly significant ($p < 0.01$), it also should be noted that their abundance and biovolume showed no regional differences (Table 2). These diminished regional changes in phytoplankton stocks between the two regions were confirmed by the vertical distribution of fluorescence showing little regional difference (Fig. 2b).

As a notable regional difference in hydrography, a prominent thermocline developed in the TR (Fig. 2a). In contrast, temperature profiles in the SA were relatively homogenous. The development of a thermocline is an important factor to initiate the spring phytoplankton bloom in this region (Mochizuki et al., 2002). From this point of view, the development of the thermocline in the TR may allow the growth of large phytoplankton, causing their dominance, the flat slope of the NBSS, and the high size diversity. On the other hand, cold surface water in the SA may mix the water column to prevent the growth of the large phytoplankton, causing the dominance of small phytoplankton and a steep NBSS slope (Table 2). Because phytoplankton size is an important factor in determining the feeding capability of zooplankton, yearly changes in thermal stratification, dominant phytoplankton size, and dominant zooplankton taxa have also been pointed out in this region (Yokoi et al., 2008).

Through the taxonomic comparison, it was notable that the

Table 3. Comparison on target biovolume (cf. Fig. 3), size range of equivalent spherical diameter (ESD), and measured volume of phytoplankton and zooplankton in this study.

Taxa	Biovolume (mm^3 $ind.^{-1}$)	Size range (ESD, μm)	Measured volume (mL)
Phytoplankton	10^{-7}–10^{-5}	4–100	1.8–3.4
Zooplankton	0.1–10	200–5000	0.35×10^6–14.1×10^6

zooplankton NBSS slope and size diversity were settled at a smaller range than those in phytoplankton (Fig. 4). Note that the scales of Fig. 4 are the same throughout the taxa/panel. Thus, zooplankton had a higher size diversity and more moderate NBSS slope than phytoplankton. These facts suggest that the regional changes in size spectra in zooplankton were smaller than those in phytoplankton. This may be due to the differences in the generation length of the two taxa. Zooplankton in this region (both SA and TR) comprise mostly large-sized *Neocalanus* copepods, which have one-year generation lengths (Yamaguchi et al., 2004, 2017 ; Matsuno and Yamaguchi, 2010 ; Fukuda et al., 2012 ; Sato et al., 2015). Their longer generation length and dominance throughout this region may have induced the similar-size spectra of the zooplankton community. On the other hand, phytoplankton generation length is short, seasonal community change is large, and regional community change in the same period has also been reported to be large (Mochizuki et al., 2002 ; Matsumoto et al., 2016). Thus, phytoplankton may exhibit a broader range of NBSS slope and size diversity than zooplankton due to differences in generation length (Fig. 4).

Future prospect

At all stations, significant NBSS regressions were obtained for both phytoplankton and zooplankton. However, there were substantial gaps in the NBSS between phytoplankton and zooplankton. The NBSS of phytoplankton ranged mainly from 10^{-7} to 10^{-5} mm^3 $ind.^{-1}$ in biovolume (Fig. 3). On the other hand, the NBSS of zooplankton ranged from 0.1 to 10 mm^3 $ind.^{-1}$ in biovolume. These discrepancies in NBSS between the two taxa were common at all stations (Fig. 3). So there was a substantial gap in biovolume between 10^{-5} and 0.1 mm^3 $ind.^{-1}$. The methods used to collect phytoplankton and zooplankton in this study may have caused this gap in the NBSS. We collected phytoplankton from 1-L water samples, made FlowCam measurements on 1.8–3.4 mL, and then targeted the 4–100 μm ESD size range. For zooplankton, we used a 335 μm mesh plankton net with a filtering volume of 22.5–28.2 m^3 (Table 1), measured ZooScan with 1/2 to 1/64 subsamples, then targeted the 0.2–5.0 mm ESD size range. Based on the above data, a large discrepancy was found between the two measurements, especially in volume ranging from 0.1×10^6 ($=0.35\times10^6$ / 3.4 in mL) to 7.8×10^6 ($=14.1\times10^6$ / 1.8 in mL) (Table 3). Through this comparison, to fill the gap between the two quantitative methods of this study, collecting approximately 5-L water samples and then gently filtering and concentrating the sample with a fine mesh (30 μm) hand net would be ideal. Or plankton collection by a gentle vertical tow of a small mouth fine mesh net (30 μm) would also cover the range.

Historically, plankton size spectra analyses targeting whole size and taxonomic ranges have been made by combining various quantitative methods (cf. Zhou, 2006 ; Irisson et al., 2022). Previous studies have combined methods from phytoplankton, zooplankton, and fishes using manual microscopy (Sprules and Stockwell, 1995) ; flow cytometry, inverted microscopy, and ZooScan (Romagnan et al., 2015) ; flow cytometry, FlowCam, and ZooScan (Zhang et al., 2019) ; flow cytometry, coulter counter, and FlowCam (Menden-Deuer et al., 2020) ; and ZooScan measurements on samples collected by two different mesh size nets (64 μm and 236 μm) (Kwong and Pakhomov, 2021). Compared with these studies, the methods of the present study, which included two categories with FlowCam measurements on small amounts of water samples and ZooScan on the net samples collected by large mesh size, contained large flaws. For this reason, our results should be treated as preliminary.

Acknowledgements

We would like to express our gratitude to the crew members of T/S *Oshoro-Maru* for their invaluable assistance in collecting the samples. We extend our sincere thanks to Ms. Shino Kumagai and Mr. Shintaro Yoshida for their help in collecting data and samples on board. The manuscript was greatly improved with the English editorial comments provided by Dr. John R. Bower. This study was supported mainly by the China Scholarship Council (20220670014). Part of this work was supported by Grant-in-Aid for Challenging Research (Pioneering) 20K20573 and Scientific Research 22H00374 (A) from the Japan Society for the Promotion of Science (JSPS).

References

Baird, M.E., Timko, P.G., Middleton, J.H., Mullaney, T.J., Cox, D.R. and Suthers, I.M. (2008) Biological properties across the Tasman Front off southeast Australia. *Deep-Sea Res. I*, **55**, 1438–1455.

Chang, F.H., Marquis, E.C., Chang, C.W. and Gong, G.C. (2013) Scaling of growth rate and mortality with size and its consequence on size spectra of natural microphytoplankton assemblages in the East China Sea. *Biogeosciences*, **10**, 5267–5280.

Espinasse, B., Carlotti, F., Zhou, M. and Devenon, J.L. (2014) Defining zooplankton habitats in the Gulf of Lion (NW Mediterranean Sea) using size structure and environmental conditions. *Mar. Ecol. Prog. Ser.*, **506**, 31–46.

Forest, A., Stemmann, L., Picheral, M., Burdorf, L., Robert, D., Fortier, L. and Babin, M. (2012) Size distribution of particles and zooplankton across the shelf-basin system in southeast Beaufort Sea : combined results from an Underwater Vision Profiler and vertical net tows. *Biogeosciences*, **9**, 1301–1320.

Fukuda, J., Yamaguchi, A., Matsuno, K. and Imai, I. (2012) Interannual and latitudinal changes in zooplankton abundance, biomass and size composition along a central North Pacific transect during summer : analyses with an Optical Plankton Counter. *Plankton Benthos Res.*, **7**, 64–74.

García-Oliva, O., Hantzsche, F.M., Maarten, B. and Wirtz, K.W. (2022) Phytoplankton and particle size spectra indicate intense mixotrophic dinoflagellates grazing from summer to winter. *J. Plankton Res.*, **44**, 224–240.

Gómez-Canchong, P., Quiñones, R.A. and Brose, U. (2012) Robustness of size-structure across ecological networks in pelagic systems. *Theor. Ecol.*, **6**, 45–56.

Gorsky, G., Ohman, M.D., Picheral, M., Stéphane G. and Prejger, F. (2010) Digital zooplankton image analysis using the ZooScan integrated system. *J. Plankton Res.*, **32**, 285–303.

Hama, N., Abe, Y., Matsuno, K. and Yamaguchi, A. (2019) Study on effect of net mesh size on filtering efficiency and zooplankton sampling efficiency using Quad-NORPAC net. *Bull. Fish. Sci. Hokkaido Univ.*, **69**, 47–56.

Herman, A.W. and Harvey, M. (2006) Application of normalized biomass size spectra to laser optical plankton counter net intercomparisons of zooplankton distributions. *J. Geophys. Res.*, **111**, C05S05.

Hikichi, H., Arima, D., Abe, Y., Matsuno, K., Hamaoka, S., Katakura, S., Kasai, H. and Yamaguchi, A. (2018) Seasonal variability of zooplankton size spectra at Mombetsu Harbour in the southern Okhotsk Sea during 2011 : An analysis using an optical plankton counter. *Reg. Stud. Mar. Sci.*, **20**, 34–44.

Huntley, M.E., Lopez, M.D.G., Zhou, M. and Landry, M.R. (2006) Seasonal dynamics and ecosystem impact of mesozooplankton at station ALOHA based on optical plankton counter measurements. *J. Geophys. Res.*, **111**, C05S10.

Irisson, J.O., Ayata, S.D., Lindsay, D.J., Karp-Boss, L. and Stemmann, L. (2022) Machine learning for the study of plankton and marine snow from images. *Annu. Rev. Mar. Sci.*, **14**, 277–301.

Jakobsen, H.H. and Carstensen, J. (2011) FlowCAM : Sizing cells and understanding the impact of size distributions on biovolume of planktonic community structure. *Aquat. Microb. Ecol.*, **65**, 75–87.

Kwong, L.E and Pakhomov, E.A. (2021) Zooplankton size spectra and production assessed by two different nets in the subarctic Northeast Pacific. *J. Plankton Res.*, **43**, 527–545.

Kydd, J., Rajakaruna, H., Briski, E. and Bailey, S. (2018) Examination of a high resolution laser optical plankton counter and FlowCAM for measuring plankton concentration and size. *J. Sea Res.*, **133**, 2–10.

Liu, Z., Li, Q.P., Ge, Z. and Shuai, Y. (2021) Variability of plankton size distribution and controlling factors across a coastal frontal zone. *Prog. Oceanogr.*, **197**, 102665.

Marcolin, C.R., Gaeta, S. and Lopes, R.M. (2015) Seasonal and interannual variability of zooplankton vertical distribution and biomass size spectra off Ubatuba, Brazil. *J. Plankton Res.*, **37**, 808–819.

Matsumoto, K., Arima, D., Matsuno, K., Yamasaki, Y., Onishi, H., Ooki, A., Hirawake, T., Yamaguchi, A. and Imai, I. (2016) The spatial and vertical distributions of a spring phytoplankton community along 155°E in the western North Pacific. *Bull. Fish. Sci. Hokkaido Univ.*, **66**, 29–38.

Matsuno, K. and Yamaguchi, A. (2010) Abundance and biomass of mesozooplankton along north-south transects (165 E and 165 W) in summer in the North Pacific : an analysis with an optical plankton counter. *Plankton Benthos Res.*, **5**, 123–130.

Menden-Deuer, S., Morison, F., Montalbano, A.L., Franz, G., Strock, J., Rubin, E., McNair, H., Mouw, C. and Marrec, P. (2020) Multi-instrument assessment of phytoplankton abundance and cell sizes in mono-specific laboratory cultures and whole plankton community composition in the North Atlantic. *Front. Mar. Sci.*, **7**, 254.

Mochizuki, M., Shiga, N., Saito, M., Imai, K. and Nojiri, Y. (2002) Seasonal changes in nutrients, chlorophyll a and the phytoplankton assemblage of the western subarctic gyre in the Pacific Ocean. *Deep-Sea Res. II*, **49**, 5421–5439.

Moore, S.K. and Suthers, I.M. (2006) Evaluation and correction of subresolved particles by the optical plankton counter in three Australian estuaries with pristine to highly modified catchments. *J. Geophys. Res.*, **111**, C05S04.

Motoda, S. (1959) Devices of simple plankton apparatus. *Mem. Fac. Fish. Hokkaido Univ.*, **7**, 73–94.

Nogueira, E., González-Nuevo, G., Bode, A., Varela, M., Morán, X.A.G. and Valdés, L. (2004) Comparison of biomass and size spectra derived from optical plankton counter data and net samples : application to the assessment of mesoplankton distribution along the Northwest and North Iberian Shelf. *ICES J. Mar. Sci.*, **61**, 508–517.

Picheral, M., Colin, S. and Irisson, J.O. (2017) EcoTaxa, a tool for the taxonomic classification of images. http://ecotaxa.obs-vlfr.fr

Reynolds, R.A., Stramski, D., Wright, V.M. and Woźniak, S.B. (2010) Measurements and characterization of particle size distributions in coastal waters. *J. Geophys. Res.*, **115**, C08024.

Romagnan, J.B., Legendre, L., Guidi, L., Jamet, Jean-Louis, Jamet, D., Mousseau, L., Pedrotti, Maria-Luiza, Picheral, M., Gorsky, G., Sardet, C. and Stemmann, L. (2015) Comprehensive model of annual plankton succession based on the whole-plankton time series approach. *PLoS One*, **10**, e0119219.

Sato, K., Matsuno, K., Arima, D., Abe, Y. and Yamaguchi, A. (2015) Spatial and temporal changes in zooplankton abundance, biovolume, and size spectra in the neighboring waters of Japan : analyses using an optical plankton counter. *Zool. Stud.*, **54**, 1–15.

Schultes, S. and Lopes, R.M. (2009) Laser Optical Plankton Counter and Zooscan intercomparison in tropical and subtropical marine ecosystems. *Limnol. Oceanogr.-Meth.*, **7**, 771–784.

Shannon, C.E. and Weaver, W.W. (1963) *The Mathematical Theory of Communications*. University of Illinois Press, Urbana.

Sourisseau, M. and Carlotti, F. (2006) Spatial distribution of zooplankton size spectra on the French continental shelf of the Bay of Biscay during spring 2000 and 2001. *J. Geophys. Res.*, **111(C5)**, C05S09.

Sprules, W.G. and Stockwell, J.D. (1995) Size-based biomass and production models in the St Lawrence Great Lakes. *ICES*

J. Mar. Sci., **52**, 705–710.

Sun, D., Chen, Y., Feng, Y.Z., Liu, Z.S., Peng, X., Cai, Y., Yu, P. and Wang, C. (2021) Seasonal variation in size diversity : Explaining the spatial mismatch between phytoplankton and mesozooplankton in fishing grounds of the East China Sea. *Ecol. Indic.*, **131**, 108201.

Suthers, I.M. (2006) Day and night ichthyoplankton assemblages and zooplankton biomass size spectrum in a deep ocean island wake. *Mar. Ecol. Prog. Ser.*, **322**, 225–238.

Teraoka, T., Amei, K., Fukai, Y., Matsuno, K., Onishi, H., Ooki, A., Takatsu, T. and Yamaguchi, A. (2022) Seasonal changes in taxonomic, size composition, and Normalised Biomass Size Spectra (NBSS) of mesozooplankton communities in the Funka Bay, southwestern Hokkaido : Insights from ZooScan analysis. *Plankton Benthos Res.*, **17**, 369–382.

Vandromme, P., Nogueira, E., Huret, M., Lopez-Urrutia, A., Sourisseau, M. and Petitgas, P. (2014) Springtime zooplankton size structure over the continental shelf of the Bay of Biscay. *Ocean Sci.*, **10**, 821–835.

Vandromme, P., Stemmann, L., Garcìa-Comas, C., Berline, L., Sun, X. and Gorsky, G. (2012) Assessing biases in computing size spectra of automatically classified zooplankton from imaging systems : A case study with the ZooScan integrated system. *Meth. Oceanogr.*, **1**, 3–21.

Yamaguchi, A., Matsuno, K., Abe, Y., Arima, D. and Imai, I. (2017) Latitudinal variations in the abundance, biomass, taxonomic composition and estimated production of epipelagic mesozooplankton along the 155ºE longitude in the western North Pacific during spring. *Prog. Oceanogr.*, **150**, 13–19.

Yamaguchi, A., Matsuno, K., Abe, Y., Arima, D. and Ohgi, K. (2014) Seasonal changes in zooplankton abundance, biomass, size structure and dominant copepods in the Oyashio region analysed by an optical plankton counter. *Deep-Sea Res. I*, **91**, 115–124.

Yamaguchi, A., Watanabe, Y., Ishida, H., Harimoto, T., Furusawa, K., Suzuki, S., Ishizaka, J., Ikeda, T. and Takahashi, M. (2002) Structure and size distribution of plankton communities down to the greater depths in the western North Pacific Ocean. *Deep-Sea Res. II*, **49**, 5513–5529.

Yamaguchi, A., Watanabe, Y., Ishida H., Harimoto,T., Furusawa, K., Suzuki, S., Ishizaka, J., Ikeda, T. and Takahashi, M.M. (2004) Latitudinal differences in the planktonic biomass and community structure down to the greater depths in the western North Pacific. *J. Oceanogr.*, **60**, 773–787.

Yokoi, Y., Yamaguchi, A. and Ikeda, T. (2008) Regional and interannual changes in the abundance, biomass and size structure of mesozooplankton in the western North Pacific in early summer analyzed using an optical plankton counter. *Bull. Plankton Soc. Japan*, **55**, 9–24.

Yurista, P., Kelly, J.R. and Miller, S. (2005) Evaluation of optically acquired zooplankton size-spectrum data as a potential tool for assessment of condition in the Great Lakes. *Environ. Manage.*, **35**, 34–44.

Zhang, W., Sun, X., Zheng, S., Zhu, M., Liang, J., Du, J. and Yang, C. (2019) Plankton abundance, biovolume, and normalized biovolume size spectra in the northern slope of the South China Sea in autumn 2014 and summer 2015. *Deep-Sea Res. II*, **167**, 79–92.

Zhou, M. (2006) What determines the slope of a plankton biomass spectrum? *J. Plankton Res.*, **28**, 437–448.

Zhou, M., Tande, K.S., Zhu, Y. and Basedow, S. (2009) Productivity, trophic levels and size spectra of zooplankton in northern Norwegian shelf regions. *Deep-Sea Res. II*, **56**, 1934–1944.